Optical properties and Raman spectra of the quasi-one-dimensional gold complexes AuX_2dibenzylsulfide ($X_2 = Cl_2, ClBr, Br_2$)

H. Tanino
*Electrotechnical Laboratory, Tsukuba, Ibaraki 305, Japan**
and Max-Planck-Institut für Festkörperforschung, D-7000 Stuttgart 80, Federal Republic of Germany

K. Takahashi, M. Tajima, M. Kato,† and T. Yao
Electrotechnical Laboratory, Tsukuba, Ibaraki 305, Japan
(Received 25 March 1988)

The compounds AuX_2dibenzylsulfide ($X_2 = Cl_2, ClBr, Br_2$) are quasi-one-dimensional (1D) halogen-bridged mixed-valence gold complexes with a sequence of -Au(I)-X-Au(III)-X- along the chains. These semiconducting compounds have been studied by absorption, reflectance, luminescence, and Raman measurements. The optical properties and Raman spectra are explained by a charge-density wave with a large Peierls gap in the Peierls-Hubbard insulator model. The Au compounds differ from related nearly ideal 1D Pt complexes by a pairing of chains. Hence, two types of charge-transfer excitons polarized parallel and perpendicular to the main chain are observed that both relax to the same self-trapped state.

I. INTRODUCTION

Quasi-one-dimensional (1D) metal complexes have been studied extensively because they exhibit a variety of low-dimensional phenomena. For example, partially oxidized tetracyanoplatinates were investigated in the search for new superconducting materials and were found to be 1D conductors with interesting electronic properties.[1] Recently, halogen-bridged mixed-valence metal complexes[2–5] (HMMC's) with alternating metal atoms and halogen atoms along the chain were found to be 1D insulators with strong electron-phonon interaction.[6] These materials have been known in the field of inorganic chemistry for a long time,[7,8] but until recently only a few comprehensive investigations of their physical properties have been performed.

Special attention has been paid to Wolffram's red salt (WRS) and its analogs with the chain of -Pt(II)-X-Pt(IV)-X-, i.e., halogen-bridged mixed-valence platinum complexes (HMPC's). The strongly polarized absorption band in the visible region is assigned to charge-transfer (CT) absorption from d_{z^2}(Pt(II)) to d_{z^2}(Pt(IV)).[7,9] Raman spectra dominated by a progression in the symmetric X-Pt-X stretching vibration[8] and a strongly Stokes-shifted broad luminescence band from the self-trapped exciton[10] were found, and the excitation and relaxation processes of the exciton were investigated in detail.[11] The optical properties of the HMPC's can be understood in terms of a 1D commensurate charge-density wave (CDW) of -$Pt^{3-\rho}$-X-$Pt^{3+\rho}$-X- ($0 < \rho \leq 1$) with double periodicity, i.e., in terms of a $2k_F$ Peierls instability of the hypothetical metallic chain -M^{3+}-X-M^{3+}-X-. In order to clarify the ground and excited states of the strongly coupled electron-phonon system, an analysis using the Peierls-Hubbard model was performed[12–14] by taking into account the electron-transfer energy, electron-phonon interaction, electron-electron correlation energy on an intrametal site, and on the nearest-neighbor site.

Extensive studies of the physical properties of HMPC's represented by the general formula $[M(II)L][M(IV)X_2L]Y_4$, where M=Pt,Pd,Ni, X=Cl,Br,I, L = (ethylamine)$_4$,(1,2-diaminoethane)$_2$,(1,2-diaminopropane)$_2$, and $Y = X \cdot H_2O, ClO_4, BF_4$,[15–32] and some theoretical investigations[33–37] have been reported. Moreover, tailored structures of metal complexes have been realized by a new technique called selective coordination epitaxy using these compounds.[38–41] All these studies were performed on the linear chains of a Pt(II)-Pt(IV) (or Pd,Ni) mixed-valence system, where the chains are decoupled by a shell of neutral ligands made up of various amines.

In this paper, we report on the optical properties of quasi-1D halogen-bridged mixed-valence gold complexes (HMGC's) AuX_2(DBS), where $X_2 = Cl_2, ClBr, Br_2$, and DBS denotes dibenzylsulfide, $S(C_7H_7)_2$. Because no other 1D mixed-valence gold complexes have been found, we use the word HMGC's to indicate the above three compounds in this paper.

In HMGC's, Au(I) and Au(III) have ligands with different coordination from that of Pt(II) and Pt(IV). We can expect that the electron-phonon system of gold complexes will be different from the nearly ideal 1D system of HMPC's. For example, the well-known three-dimensional (3D) crystal $Cs_2Au(I)Au(III)Cl_6$ has a perovskitelike structure with two types of linear chains of -$Au^{2-\rho}$-X-$Au^{2+\rho}$-X- ($0 < \rho \leq 1$) having different lengths along the a and c axes.[42,43] The quasi-1D HMGC's have an intermediate structure between the nearly ideal 1D HMPC's and the 3D $Cs_2Au(I)Au(III)Cl_6$, and are expected to have intermediate properties. By comparing HMGC's with HMPC's, common features and varieties of 1D HMMC's will be clarified.

Interrante *et al.*[44] measured the conductivity of $AuCl_2$(DBS) and $AuBr_2$(DBS) under pressure up to 30 GPa. This study was performed in a series of investigations to search for conductive 1D materials using high-pressure techniques[45,46] and was the only report on the physical properties of HMGC's until now.

Here, we report on absorption, reflectance, luminescence, and Raman-scattering studies of $AuCl_2$(DBS), AuClBr(DBS), and $AuBr_2$(DBS). In Sec. II we first give a brief summary of crystal-structure data. The experimental procedure and results are presented in Secs. III and IV, and a discussion of the experimental data in terms of a charge-density wave $-Au^{2-\rho}$-X-$Au^{2+\rho}$-X- $(0<\rho\leq 1)$ is given in Sec. V.

II. CRYSTAL STRUCTURE

Preliminary structure determinations of $AuCl_2$(DBS) and $AuBr_2$(DBS) were reported by Brain *et al.* in 1952.[47] They suggested that $AuCl_2$(DBS) and $AuBr_2$(DBS) are made of the main chain of -Au(I)-X-Au(III)-X- as shown in Fig. 1, and represented by the following expression: [Au(I)X'(DBS)][Au(III)X_2X'(DBS)], where X and X' denote Cl in $AuCl_2$(DBS) and X and X' denote Br in $AuBr_2$(DBS), respectively. Recently, an x-ray crystal-structure determination of $AuCl_2$(DBS) has been performed by Takahashi *et al.*[48] which confirms Brain's proposed chain structure. Here we briefly summarize structural properties of $AuCl_2$(DBS).

Throughout this paper, we use the coordinates x, y, and z defined in Fig. 2. The direction of the main chain of -Au(I)-X-Au(III)-X- is along the x axis. Figure 2(a) shows a local crystal structure made of two chains of $AuCl_2$(DBS) viewed along the x axis. Figures 2(b) and 2(c) show these two chains in y- and z-axis projection, respectively. In the chain of $AuCl_2$(DBS), the almost square planar configuration of the ligands around Au(III) is not oriented perpendicular to the chain direction as in HMPC's, but lies in the xy plane which includes the chain axis. Here, only two ligands of DBS and halogen X' surround the chain. As shown in Fig. 2, a ribbonlike sheet structure is built from the coordinating planes, and two sheets of neighboring chains face each other in the crystal. These two chains are surrounded by the neutral ligands of DBS and, thus, the electron-phonon system of the two chains is shielded from the effect of other chains. The bridging chlorines are positioned close to the golds in the neighboring chain, and a ladderlike mixed-valence network is realized as seen in Fig. 2(b). This network is intermediate between the 1D chain structure of HMPC's and the 3D network of $Cs_2Au(I)Au(III)Cl_6$.

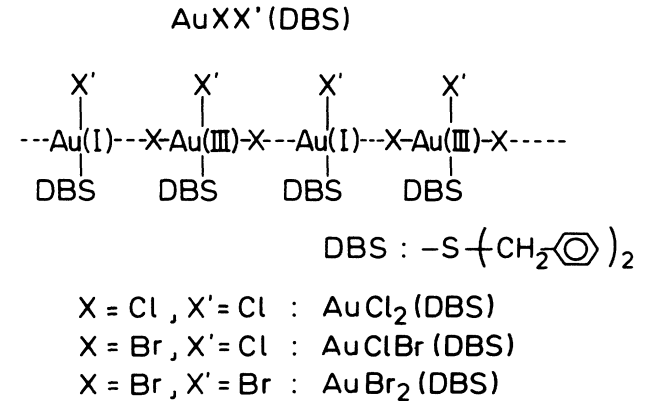

FIG. 1. Schematic of one chain of -X-Au(I)-X-Au(III)- in AuX_2(DBS), where $X_2=Cl_2$,ClBr, Br_2 (Refs. 47 and 48). In the case of AuClBr(DBS), Br is always on the main chain (Ref. 49).

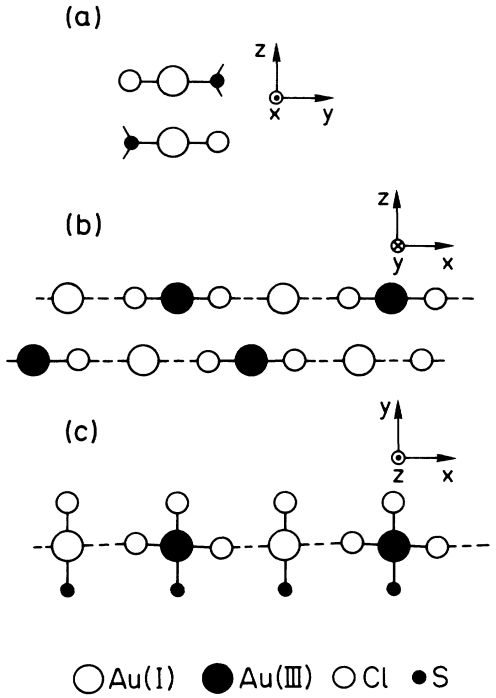

FIG. 2. Crystal structure of $AuCl_2$(DBS) (Ref. 48). (a) A local crystal structure made of two chains which is seen along the x axis. Ligands of DBS are surrounding the chains to separate them from the other pairs of chains. (b) Relative arrangement of two chains seen from the y direction. (c) A view of one chain from the z direction. The shift of the bridging halogens in the y direction from the main axis does not change the discussions.

The chain axis x is along the a crystal axis, but the y and z axes have different orientations in the crystal depending on the chain. So, we cannot assign y to b and z to c. This uncertainty explains the fact that no difference has been found between the spectra for two different polarizations of incident light $\mathbf{E}\|\mathbf{b}$ and $\mathbf{E}\|\mathbf{c}$ in absorption, reflectance, luminescence, and Raman measurements. In this paper, we only distinguish between $\mathbf{E}\|\mathbf{x}$ and $\mathbf{E}\perp\mathbf{x}$.

The crystal data of $AuCl_2$(DBS) are as follows:[48] It is a monoclinic system with the space group $P2_1/c$, $a=5.69$ Å, $b=19.93$ Å, $c=13.43$ Å, $\beta=93.3°$. The distance between Au(I) and Au(III) in the main chain is 5.69 Å. The distance between the chains is 3.32 Å. The distances between Au(III) and Cl in the main chain are 2.26 and 2.32 Å with the average of 2.29 Å. The distances between Au(I) and Cl in the main chain are 3.37 and 3.44 Å with

the average of 3.41 Å. The shortest distance from Au to the Cl in the neighboring chain is 3.42 Å.

The structures of $AuBr_2$(DBS) (Ref. 47) and AuClBr(DBS) (Ref. 49) were proposed to have similar chains of -Au(I)-*X*-Au(III)-*X*- as $AuCl_2$(DBS). In the case of AuClBr(DBS), it is also proposed by x-ray-absorption spectroscopy that the halogen in the main chain *X* is Br and the side ligand halogen *X'* is Cl.[49] Moreover, in the following discussion, we assume that the coupled-chain structure of $AuCl_2$(DBS) is also realized in $AuBr_2$(DBS) and AuClBr(DBS).

III. EXPERIMENTAL PROCEDURE

The samples of the gold complexes were prepared in the form of crude crystals by using methods described in the literature.[47,50–52] They were recrystallized from chloroform-diethylether solutions, and single crystals were obtained as orange-red needles for $AuCl_2$(DBS), brown needles for AuClBr(DBS), and deep-brown needles for $AuBr_2$(DBS). They are dichromatic crystals with a length of 0.1–2 mm, and a width of 0.01–0.1 mm. The colors of AuClBr(DBS) and $AuBr_2$(DBS) are dark red parallel to the needle axis, and red perpendicular to it, and the color of $AuCl_2$(DBS) is orange and light orange, respectively. The change of the color of $AuCl_2$(DBS) with polarization direction is much less than in AuClBr(DBS), $AuBr_2$(DBS), and HMPC's. The main chain of -$Au^{2-\rho}$-*X*-$Au^{2+\rho}$-*X*- is confirmed to be always parallel to the needle axis. All measurements were performed on single crystals. Absorption measurements were performed using a microspectrophotometer.[53] The procedure for the luminescence measurements is described elsewhere.[54] Raman spectra were measured with a 0.75-m double monochromator and a standard photon-counting system. Raman and luminescence spectra were taken in a backscattering configuration at 4 K. Samples were directly immersed in liquid helium. The power of the exciting radiation from the argon-ion laser was kept sufficiently low to avoid damaging the samples, which are less stable than HMPC's.[11]

IV. EXPERIMENTAL RESULTS

Polarized absorption spectra at room temperature for three HMGC's are shown in Fig. 3. All compounds show similar tails of the absorption bands both in the case of E||x and E⊥x. This is quite different from all HMPC's, which only have weak or nonexistent absorption bands for E⊥x in the visible region. In all three compounds, the energies of the absorption edge for E⊥x are higher than those for E||x. The energy of the edge decreases in the order of $AuCl_2$(DBS), AuClBr(DBS), and $AuBr_2$(DBS) for each polarization. For comparison, the absorption edges of the control compounds of Au(III)Cl_3(DBS) and Au(III)Br_3(DBS) are also indicated in Fig. 3.

The luminescence spectra of these compounds at 4 K are also shown in Fig. 3. The spectra of AuClBr(DBS) and $AuBr_2$(DBS) are Gaussian-like broad luminescence bands similar to those of HMPC's. In the spectra of $AuCl_2$(DBS) two bands are observed. The lower band

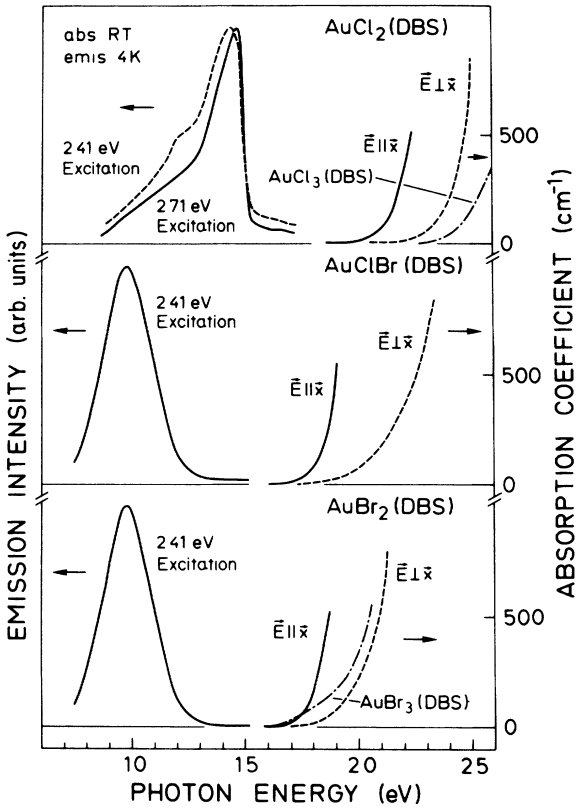

FIG. 3. Polarized absorption spectra at room temperature and luminescence spectra excited at 2.41 eV [and 2.71 eV in $AuCl_2$(DBS)] at 4 K of $AuCl_2$(DBS), AuClBr(DBS), and $AuBr_2$(DBS). The absorption edges of the control compounds of Au(III)Cl_3(DBS) and Au(III)Br_3(DBS) are also shown.

peaked at around 1.2 eV increases in intensity when the sample was damaged by irradiation. The peak at around 1.45 eV shifts to higher energy by increasing the excitation energy as observed in some HMPC's.[11,17] All the luminescence spectra have large Stokes shifts relative to the absorption edges. The degree of polarization of the luminescence band of $AuCl_2$(DBS) is smaller than those of AuClBr(DBS) and $AuBr_2$(DBS) as shown in Table I.

Figure 4 shows the polarized reflectivity of these compounds at room temperature. The oscillating structure in $AuCl_2$(DBS) and the increase of the reflectivity of AuClBr(DBS) and $AuBr_2$(DBS) in the low-energy region below 2 eV are due to interference produced by reflection from the back face of the transparent crystals. The reflectance spectra of AuClBr(DBS) and $AuBr_2$(DBS) in E||x show a broad peak of similar shape to that observed in HMPC's.[15,17,39] The peak of $AuCl_2$(DBS) for E||x is very weak. In all three compounds no corresponding peaks were observed for E⊥x.

The shape of the absorption edge and reflectance peak of AuClBr(DBS) and $AuBr_2$(DBS) looks like that of some HMPC's. We can speculate from the shape that the bands in HMGC's are due to one broad oscillator similar to HMPC's. Unfortunately, Kramers-Kronig transfor-

TABLE I. Summary of optical properties. E_{th} denotes the threshold energy of absorption spectra defined as the energy where $\alpha=500\ cm^{-1}$. E_R denotes the peak energy of the reflectance spectra. f denotes the estimated oscillator strength by a model oscillator. E_1 denotes the peak energy of the luminescence spectra. ΔE_1 denotes the full width at half maximum of the luminescence. I_1, I_2, I_3, and I_4 denote the intensity of the luminescence in each polarization of incident light $\mathbf{E}_i$ and luminescence $\mathbf{E}_l$, where $I_1=100$. $P_\parallel$ and $P_\perp$ denote the degree of polarization defined by $P_\parallel=(I_1-I_2)/(I_1+I_2)$ and $P_\perp=(I_3-I_4)/(I_3+I_4)$.

	$AuCl_2$(DBS)	AuClBr(DBS)	$AuBr_2$(DBS)
E_{th} ($\mathbf{E}\parallel\mathbf{x}$) (eV)	2.24	1.90	1.87
E_{th} ($\mathbf{E}\perp\mathbf{x}$) (eV)	2.48	2.26	2.09
E_R ($\mathbf{E}\parallel\mathbf{x}$) (eV)	2.63	2.27	2.21
f ($\mathbf{E}\parallel\mathbf{x}$)	0.2	0.5	0.6
E_1 (eV)	1.45	0.98	0.98
ΔE_1 (eV)	0.2	0.25	0.25
I_1 ($\mathbf{E}_i\parallel\mathbf{x}\parallel\mathbf{E}_l$)	100	100	100
I_2 ($\mathbf{E}_i\parallel\mathbf{x}\perp\mathbf{E}_l$)	70	53	43
I_3 ($\mathbf{E}_i\perp\mathbf{x}\parallel\mathbf{E}_l$)	79	65	89
I_4 ($\mathbf{E}_i\perp\mathbf{x}\perp\mathbf{E}_l$)	62	38	38
$P_\parallel$	0.18	0.31	0.40
$P_\perp$	0.12	0.26	0.40
E_l/E_R	0.55	0.43	0.44

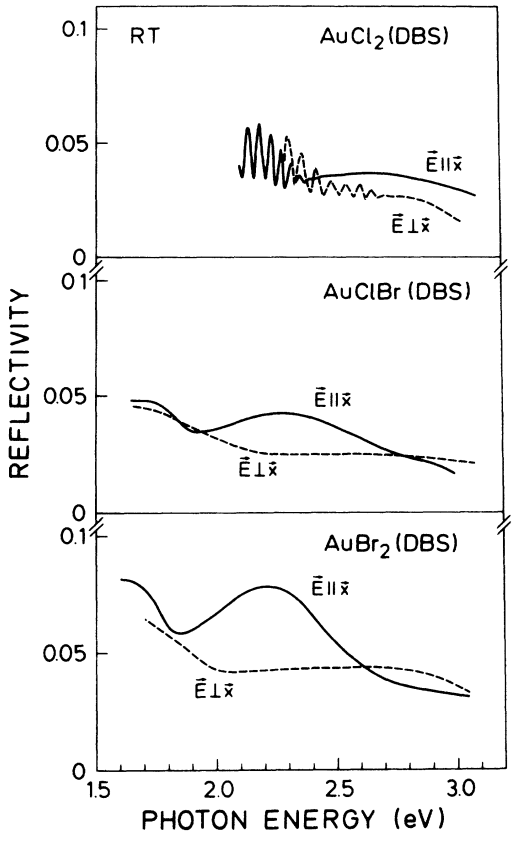

FIG. 4. Polarized reflectance spectra at room temperature of $AuCl_2$(DBS), AuClBr(DBS), and $AuBr_2$(DBS).

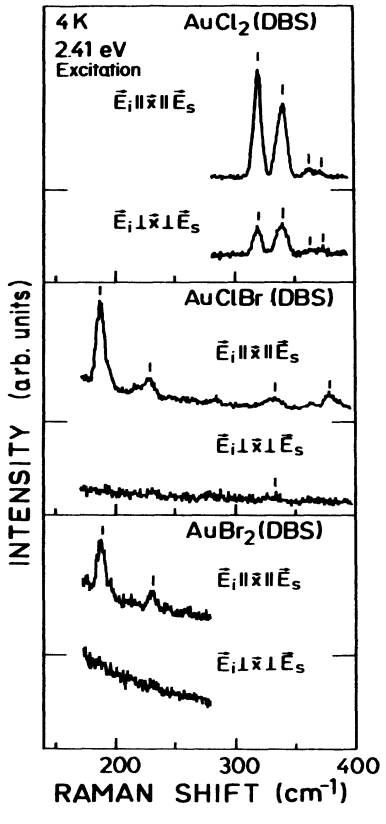

FIG. 5. Polarized Raman spectra excited at 2.41 eV at 4 K of $AuCl_2$(DBS), AuClBr(DBS), and $AuBr_2$(DBS). The electric fields of incident light $\mathbf{E}_i$ and scattered light $\mathbf{E}_s$ were chosen to be parallel to the main chain ($\parallel\mathbf{x}$) and perpendicular to the chain ($\perp\mathbf{x}$). No signal was observed in the cases of $\mathbf{E}_i\parallel\mathbf{x}\perp\mathbf{E}_s$ and $\mathbf{E}_i\perp\mathbf{x}\parallel\mathbf{E}_s$.

TABLE II. Raman peaks at 4 K. The energies of 319- and 339-cm^{-1} modes are 318 and 338 cm^{-1} at room temperature, respectively (Ref. 56). The assignments are described in Sec. IV B.

Raman peaks (cm^{-1})			
$AuCl_2$(DBS)	AuClBr(DBS)	$AuBr_2$(DBS)	Assignment
	188	189	ν_s(Br-Au(III)-Br)
	229	232	
319			ν_s(Cl-Au(III)-Cl)
339	332		ν_s(S-Au-Cl)
361			
370			

mation as reported before[17,21] is impossible because of the narrow spectral range. However, a least-squares analysis using a model oscillator is useful to estimate the magnitude of the oscillator strength, f, of the charge-transfer absorption band in HMMC's.[16] We summarize the estimated values of f in Table I. The oscillator strengths of AuClBr(DBS) and $AuBr_2$(DBS) for $\mathbf{E}\|\mathbf{x}$ are larger than $AuCl_2$(DBS). An increase is also observed from AuClBr(DBS) to $AuBr_2$(DBS). However, all these values are much smaller than $f=3-7$ as observed in some HMPC's.[17,21] In the cases of $\mathbf{E}\perp\mathbf{x}$, the analysis gives an upper limit for f as 0.1 in three compounds. The spectra in Fig. 3 show that the absorption coefficient α at the peak of the absorption band is larger than 1000 cm^{-1}, so we can estimate a lower limit for f from this value as 0.03. The oscillator strength for $\mathbf{E}\|\mathbf{x}$ in $AuCl_2$(DBS), 0.2, is of the same order as for $\mathbf{E}\perp\mathbf{x}$.

In Table I, relevant energies are summarized of absorption edges, reflectance peaks, and luminescence peaks. The relative intensities when the electric fields of the incident light $\mathbf{E}_i$ and the luminescence $\mathbf{E}_l$ are polarized parallel or perpendicular to the chain direction x are also given in Table I. The intensity in $\mathbf{E}_i\|\mathbf{x}\|\mathbf{E}_l$ was set to 100. The degree of polarization P calculated from these data is also shown. These values are much smaller than that of WRS, where $P_{\|}=P_{\perp}=0.8$.[11]

Figure 5 shows the polarized Raman spectra of the three compounds excited at 2.41 eV at 4 K. No signal was found in the other configurations of $\mathbf{E}_i\|\mathbf{x}\perp\mathbf{E}_s$ and $\mathbf{E}_i\perp\mathbf{x}\|\mathbf{E}_s$, where $\mathbf{E}_i$ and $\mathbf{E}_s$ are the incident light and the scattered light, respectively. The observed phonon modes indicated by small bars in Fig. 5 are summarized in Table II. We assign the modes by referring to the spectra of related compounds such as Au(III)Cl_3(DBS) as discussed in Sec. IV B.

V. DISCUSSION

A. Charge-transfer exciton absorption

The control compounds Au(I)Cl(DBS) and Au(I)Br(DBS) have no absorption bands in the visible region. On the other hand, Au(III)Cl_3(DBS) and Al(III)Br_3(DBS) have absorption bands as shown in Fig. 3. However, they are assigned to be internal charge-transfer transitions from halogen to Au(III).[55] These assignments are confirmed by the pressure dependence of the absorption edges; the shift of these control compounds is much less than that of HMGC's. The details of high-pressure studies will be published in separate papers.[56,57] We can conclude that all of the absorption bands of HMGC's shown in Fig. 3 originate from the mixed-valence configuration of HMGC's with Au(I) and Au(III) in a similar manner as in HMPC's with Pt(II) and Pt(IV). The existence of the broad luminescence band shows that the absorption in HMGC's should also be assigned to exciton absorption, because the luminescence can only appear if the electron and hole are combined by Coulomb interaction.[6] From the large Stokes shift of the luminescence we speculate that halogen atoms are strongly distorted towards the middle point of the gold atoms in the self-trapped state.[11] The terms charge-transfer exciton (CTE) and self-trapped exciton (STE) will be used from now on.

In the case of HMPC's, the visible absorption is assigned to the charge-transfer exciton transition from the occupied d_{z^2}(Pt(II)) to the unoccupied d_{z^2}(Pt(IV)) by way of $p_z(X)$ orbitals. The electronic state of the CTE in HMGC's is assigned as follows: The occupied state of HMPC's is d^8(Pt(II)) and d^6(Pt(IV)), but that of HMGC's is d^{10}(Au(I)) and d^8(Au(III)). In the coordinate system defined in Fig. 2, the quasisquare plane of the ligands X_3(DBS) around Au(III) lies in the xy plane which includes the chain axis. In considering the surroundings of Au(I) ions, the halogens in the neighboring chain can be ignored because they are a little farther than the bridging halogens in the chain. So, the Au(I) ion has the deformed square planar configuration made of the ligands X(DBS) of Au(I) and the bridging halogens, and is considered to have approximately the same coordination geometry as the Au(III) ion. The $d_{x^2-y^2}$ orbital of Au(III) and Au(I) will be repelled by the ligands, and will be the top of the valence band for Au(I) and the bottom of the conduction band for Au(III).[44,45] Thus, we assign the absorption band for $\mathbf{E}\|\mathbf{x}$ as the transition from $d_{x^2-y^2}$(Au(I)) to $d_{x^2-y^2}$(Au(III)) by way of the $p_x(X)$ orbital, where X represents the bridging chlorine atom in the main chain as shown in Fig. 6.

Moreover, a visible absorption band for $\mathbf{E}\perp\mathbf{x}$ is observed in contrast to HMPC's. This band shifts to lower energy when changing halogen atoms, in a similar way as the band for $\mathbf{E}\|\mathbf{x}$. The luminescence from the self-trapped state is also observed by exciting this band. Thus, we assign them also to charge-transfer exciton absorption which is observed only in the coupled-chain structure. In the case of the ideal 1D system such as

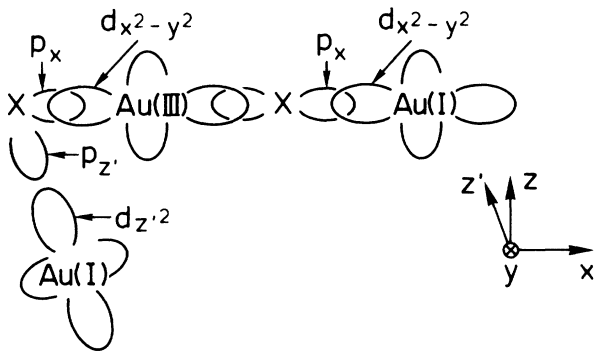

FIG. 6. Schematic of the two types of electron-transfer mechanism expected in the coupled chain of $AuCl_2(DBS)$ from Au(I) to Au(III) by way of X. Both principal transfer on the main chain and transfer to the neighboring chain are shown.

HMPC's, no electric dipole perpendicular to the chain direction will be created by charge transfer between the mixed-valence metals, but in the coupled-chain system, it will appear by transferring electrons between the chains. For example, the d_{z^2} and d_{zx} orbitals of Au(I) are below the $d_{x^2-y^2}$ orbital and have a small overlap with the p_z orbital of the chlorine in the neighboring chain, because of the short distance between Au(I) and Cl, 3.42 Å. Here, the position of the chlorine is tilted from the z direction of Au(I). Hence, the $d_{z'^2}$ state of Au(I), which is the mixture of the d_{z^2} and d_{zx} orbitals, is transferred to the unoccupied $d_{x^2-y^2}$(Au(III)) by the mixture of p_z and p_x orbitals, $p_{z'}$, as shown in Fig. 6.

Comparing $AuBr_2(DBS)$ with $AuCl_2(DBS)$, the absorption edge for both $\mathbf{E}\|\mathbf{x}$ and $\mathbf{E}\perp\mathbf{x}$ shifts to lower energy by the same degree. This tendency is explained by the difference in the ionic radius between Br and Cl. Increasing the radius, the overlap integral between $d_{x^2-y^2}$(Au(I)) and $p_x(X)$ or between $d_{z'^2}$(Au(I)) and $p_z(X)$ will increase. The increase of the interaction between Au(I) and X causes the shift of the halogen to the middle point of the gold atoms and reduces the differences in the electron distribution ρ of the charge-density wave $-Au^{2-\rho}$-X-$Au^{2+\rho}$-X-.

In AuClBr(DBS), as shown by x-ray-absorption spectra,[49] all bromines are on the main chain, and all chlorines are in the y direction. This is supported by absorption, reflectance, and luminescence spectra. The absorption edge and reflectance peak for $\mathbf{E}\|\mathbf{x}$ in AuClBr(DBS) resemble more closely $AuBr_2(DBS)$ than $AuCl_2(DBS)$. The luminescence of AuClBr(DBS) is quite similar to $AuBr_2(DBS)$.

The difference of the absorption spectra between AuClBr(DBS) and $AuBr_2(DBS)$ can be explained qualitatively. Replacing Br by Cl coordinated in y direction of Au(I), the repulsion from the halogens to the occupied $d_{x^2-y^2}$ and d_{z^2} states decreases, and the extent of the orbital in the z and x directions will decrease slightly. Hence, the transfer integral between halogens and Au(III) decreases, and the energy gap of AuClBr(DBS) will be larger than $AuBr_2(DBS)$.

B. Raman study of resonant phonons

The assignment of the phonons summarized in Table II is performed as follows: In $AuCl_2(DBS)$, the mode strongly resonant to the CTE should be assigned to the symmetric stretching vibration of the halogen atoms around Au(III) in the main chain ν_s(Cl-Au(III)-Cl), because this is just the Peierls distortion in the 1D system. However, since $d_{x^2-y^2}$ of Au(I) and Au(III) of the CTE in the main chain has electron density in the y direction, another phonon of the symmetric stretching vibration in the y direction ν_s(S-Au(III)-Cl) and ν_s(S-Au(I)-Cl) may also show the resonance. Another CTE perpendicular to the main chain along the z direction will also assist it. Hence, we see two strong peaks in the spectra of $AuCl_2(DBS)$. From the polarization dependence of the intensity of 319 cm^{-1} and 339 cm^{-1}, the former being more resonant in the x direction is assigned to ν_s(Cl-Au(III)-Cl) and the latter to ν_s(S-Au-Cl). Allen and Wilkinson[58] oppositely assigned the two modes at around 315 cm^{-1} and 340 cm^{-1} in Au(III)Cl_3L. [$L=S(CH_3)_2$, $S(C_2H_5)_2$, etc.] However, the only reason for this assignment was because the value of 340 cm^{-1} is similar to the a_{1g} mode in $AuCl_4^-$ ions. Our assignment is supported by the following discussion on other compounds, and also by the pressure effect.[57]

In AuClBr(DBS), all bromines are on the main chain, and all chlorines are in the y direction as introduced in Sec. II. Hence, ν_s(S-Au-Cl) and ν_s(Br-Au(III)-Br) must be observed, but ν_s(S-Au-Br) and ν_s(Cl-Au(III)-Cl) should be missing. The mode at 332 cm^{-1} assigned as ν_s(S-Au-Cl) in Table II is in agreement with the value for $AuCl_2(DBS)$. The mode at 188 cm^{-1} should be related to the stretching vibration of Au-Br ν_s(Br-Au(III)-Br) as shown in Table II. In $AuBr_2(DBS)$, the mode at 189 cm^{-1} is assigned to ν_s(Br-Au(III)-Br) referring to AuClBr(DBS).

Strongly observed modes of HMPC's are stretching vibrations of Pt-X which are expected to be resonant to the CTE.[8] This tendency was confirmed also in HMGC's. The polarization dependence of AuClBr(DBS) and $AuBr_2(DBS)$ is very different from $AuCl_2(DBS)$. Only ν_s(S-Au-Cl) in AuClBr(DBS) appears weakly also for $\mathbf{E}_i\perp\mathbf{x}$, but all others are observed only for $\mathbf{E}_i\|\mathbf{x}$. This is discussed in the following section.

C. Charge-density wave in HMGC's

The mixed-valence chain structure of -Au(I)-X-Au(III)-X- is considered to be a 1D CDW of $-Au^{2-\rho}$-X-$Au^{2+\rho}$-X-. In this picture, a Peierls distortion, which is the distortion of the halogen from the middle point between Au(I) and Au(III), is related to the amplitude of the CDW ρ. We calculate the renormalized Peierls distortion δ defined by $(d_2-d_1)/(d_1+d_2)$, where d_1 and d_2 are the distance between Au(III) and X and the distance between Au(I) and X as shown in Table III. The values for $AuCl_2(DBS)$ are calculated from our crystal data,[48] and those for AuClBr(DBS) and $AuBr_2(DBS)$ from our lattice data.[59] The values of d_2 are substituted by the distance between Au(III) and Br in the control compound

TABLE III. Atomic distances along the chain and renormalized Peierls distortion δ. $d_1 = d$(Au(III)-X), d_2(Au(I)-X), and $d_1 + d_2 = d$(Au(III)-Au(I)).

	d_1+d_2	d_1	d_2	$\delta = d_2 - d_1 / d_1 + d_2$
$AuCl_2$(DBS)[a]	5.69	2.29[b]	3.40[b]	0.20
AuClBr(DBS)	5.72[a]	2.42[c]	3.30	0.15
$AuBr_2$(DBS)	5.76[a]	2.42[c]	3.34	0.16
WRS[d]	5.39	2.26	3.13	0.16
Pt(en)Cl[e]	5.40	2.32	3.09	0.14

[a]Reference 48.

[b]The chlorines in the 1D chain have two positions with the occupancy factors of 0.5 (Ref. 48). The averaged values shown here are enough for the present discussion.

[c]The value of the distance between Au and Br in Au(III)Br_3 (DBS) was used (Ref. 59).

[d]WRS denotes Wolffram's red salt, $[Pt(II)(EA)_4][Pt(IV)Cl_2(EA)_4]Cl_4 \cdot 4H_2O$, where EA denotes ethylamine, $C_2H_5NH_2$, Ref. 61.

[e]Pt(en)Cl, $[Pt(II)(en)_2][Pt(IV)Cl_2(en)_2](ClO_4)_4$, where en denotes 1,2-diaminoethane, $NH_2CH_2CH_2NH_2$, Ref. 62.

Au(III)Br_3(DBS).[60] This assumption is enough for a rough estimate of δ, because the value of d_1 in HMMC's does not change much depending on the compound. Since the fluctuation of d_1 is less than 5% in all gold or platinum compounds, the error in δ should be less than 10%. The enhancement of the oscillator strength from $AuCl_2$(DBS) to $AuBr_2$(DBS) and AuClBr(DBS) for $\mathbf{E}\|\mathbf{x}$ is explained by the increase of the electron transfer T in the 1D chain. As δ decreases, the Peierls gap which is proportional to the absorption edge E_{th} will decrease.

Both the absorption band and the luminescence band of $AuCl_2$(DBS) are at higher energies than those of $AuBr_2$(DBS) and AuClBr(DBS), respectively. Since the absorption peak E_{ab} of the CTE is expected to be close to the reflectance peak E_R with the deviation of less than 0.2 eV as seen in HMPC's,[39] we can substitute E_l/E_R for E_l/E_{ab}. The values of all three compounds are around 0.5, as in HMPC's. This can be explained as follows: Even though the exchange of halogens causes an increase in the transfer energy T, it also changes the electron-phonon interaction S, the electron-electron correlation energy on an intrametal site U, and on the nearest-neighbor site V. In other words, the absolute energy scale should be renormalized by the characteristic energy of each chemical species such as T. The peak energy of luminescence E_l of the Peierls-Hubbard system is roughly given by $3V - U$ almost independent of T.[63] Thus, the invariability of E_l/E_R $[\propto (3V-U)/T]$ indicates the change of the absolute values of V (and U) relative to T. This result is consistent with the result on HMPC's with the bridging halogens of Cl, Br, and I.[17]

AuClBr(DBS) and $AuBr_2$(DBS) with the same bridging halogens in the main chain show slightly different CTE absorption but similar luminescence. The former can be explained by the change of δ of the Peierls system and the latter by the intrinsic U and V of the localized STE. The role of the exchange of the side halogen from Cl to Br simply causes an internal lattice pressure on the CDW without changing any parameters other than the electron transfer T. This explanation is quite consistent with the explanation of the pressure effect in Wolffram's red salt (WRS).[23]

The normalized Peierls distortion δ in $AuCl_2$(DBS) of 0.20 is much larger than that of $AuBr_2$(DBS), AuClBr(DBS), and some of HMPC's. This large value explains the relatively weak oscillator strength and the isotropic nature of the polarized Raman spectra. On the other hand, in AuClBr(DBS) and $AuBr_2$(DBS) with bromines as bridging halogens, as the electron transfer between Au(I) and X increases, the oscillator strength f for $\mathbf{E}\|\mathbf{x}$ is enhanced enormously. The fact that the Raman spectra of AuClBr(DBS) and $AuBr_2$(DBS) are strongly polarized in $\mathbf{E}\|\mathbf{x}$ appears reasonable, because the resonant effect is proportional to the oscillator strength. The absolute values of f, 0.5 in AuClBr(DBS) and 0.6 in $AuBr_2$(DBS), are smaller than those of HMPC's. For example, $f = 3.0$ (Ref. 17) or 2.8 (Ref. 21) in Pt(en)Cl, $[Pt(II)(en)_2][Pt(IV)Cl_2(en)_2](ClO_4)_4$ (en denotes 1,2-diaminoethane), where $\delta = 0.14$ as shown in Table III. This might be explained by much weaker electron transfer for $d_{x^2-y^2}$ (Au) than d_{z^2} (Pt). On the other hand, the absorption edges for $\mathbf{E}\|\mathbf{x}$ in both $AuBr_2$(DBS) and WRS, where $\delta = 0.16$ as shown in Table III, are close to 1.9 eV.[11] We suggest that the absorption edges of all HMMC's are essentially determined only by the absolute value of δ, independent of the chemical species. We conclude that the CDW picture is generally applicable in the Au(I)-Au(III) mixed-valence system and the M(II)-M(IV) (M=Pt,Pd,Ni) system.

D. Self-trapped exciton (Refs. 11 and 64)

The relaxation process in the coupled-chain structure of HMGC's compared with that of the ideal 1D system of HMPC's is an interesting problem. Even though absorption spectra show large differences in polarization, the luminescence of the STE in HMGC's is a single band in each compound, and shows no dependence on polarization of incident light. It indicates that the STE associated with the two types of charge-transfer excitons is one localized state with one definite electron-hole distribution. Since no difference in the luminescence was observed between AuClBr(DBS) and $AuBr_2$(DBS) whose bridging halogens are Br, the side halogens are not related to it. The degree of polarization P of the luminescence from the self-trapped state informs us the distribution of wave functions of the STE. Since P of HMGC's, especially of $AuCl_2$(DBS), is much less than 0.8 found in WRS,[11] the STE's are less one dimensional as observed in the self-trapped states of three-dimensional materials such as alkali halides.[64] Therefore, we suggest that the halogens of both neighboring chains are deformed simultaneously, and the size of the STE in the chain direction is not so large as compared with the size perpendicular to the chain direction in the order of the distance between the neighboring chains. This less one-dimensional nature should not be observed in the single-chain system of

HMPC's, where the size of the STE perpendicular to the chain direction must be small. The increase in the degree of polarization of the luminescence from $AuCl_2$(DBS) to AuClBr(DBS) and $AuBr_2$(DBS) is due to the increase of 1D nature of the electronic state of the STE induced by changing the bridging halogens, because electron transfer by way of the $p_x(X)$ orbital increases in proportion to the ionic radius of bridging halogens. The shift of the luminescence band of $AuCl_2$(DBS) by changing the excitation energy shows that the self-trapped state might have a variety of microscopic origins as suggested in some HMPC's.[11,17]

VI. CONCLUSION

We have studied three 1D halogen-bridged mixed-valence gold complexes (HMGC's) of AuX_2(DBS) ($X_2=Cl_2$,ClBr,Br_2) by absorption, reflectance, luminescence, and Raman measurements. The optical properties are discussed in terms of a charge-density wave with a large Peierls gap in the Peierls-Hubbard insulator model. Our results are summarized as follows.

(i) The picture of the commensurate CDW and the Perierls-Hubbard model which was applied to halogen-bridge mixed-valence platinum complexes (HMPC's) with Pt(II) and Pt(IV) can also explain the electron-phonon system of HMGC's with Au(I) and Au(III).

(ii) The unique structure with a pairing of chains in HMGC's causes different properties compared to HMPC's. Two types of charge-transfer absorption bands are observed, polarized with $\mathbf{E}\|\mathbf{x}$ as in HMPC's and also with $\mathbf{E}\perp\mathbf{x}$.

(iii) The differences between $AuCl_2$(DBS) and $AuBr_2$(DBS) originate from the chemical exchange of the bridging halogens, and the difference between AuClBr(DBS) and $AuBr_2$(DBS) can be explained as an internal lattice pressure effect on the CDW. This explains the unresolved problem of the inconsistency of chemical exchange and pressure effect in HMPC's.

(iv) The one-dimensional nature is weaker than in HMPC's due to the $d_{x^2-y^2}$ orbital in Au(I)-Au(III) being less effective in electron transfer than the d_{z^2} orbital in Pt(II)-Pt(IV). For example, the oscillator strength of the 1D charge-transfer exciton and the resonant enhancement of Raman spectra is smaller than in HMPC's.

(v) The self-trapped state is less one dimensional than in HMPC's, because of the coupled-chain structure. Both charge-transfer excitons for $\mathbf{E}\|\mathbf{x}$ and $\mathbf{E}\perp\mathbf{x}$ relax to the same self-trapped state.

ACKNOWLEDGMENTS

The authors are grateful to L. V. Interrante, K. Syassen, S. Abe, and R. L. Johnson for helpful advice and comments. They also thank T. Ishiguro and M. Cardona for their continuous interest and encouragement.

---

*Permanent address.

†On leave from Stanley Electric Co., Midori-ku, Yokohama 227, Japan.

[1]See, for exámple, H. J. Keller, in *Extended Linear Chain Compounds,* edited by J. S. Miller (Plenum, New York, 1982), Vol. 1, p. 357.

[2]H. Wolffram, Dissertation, University of Königsberg, Königsberg, Germany, 1900 (unpublished).

[3]H. Reihlen and F. Flohr, Ber. Dtsch. Chem. Ges. **67**, 2010 (1934).

[4]S. Kida, Bull. Chem. Soc. Jpn. **38**, 1804 (1965).

[5]N. Matsumoto, M. Yamashita, and S. Kida, Bull. Chem. Soc. Jpn. **51**, 2334 (1978).

[6]K. Kobayashi, in *Excitonic Processes in Solids,* Vol. 60 of *Springer Series of Solid-State Sciences,* edited by M. Ueta, H. Kanzaki, K. Kobayashi, Y. Toyozawa, and E. Hanamura (Springer, Berlin, 1986), p. 475.

[7]See, for example, P. Day, in *Low-Dimensional Cooperative Phenomena,* edited by H. J. Keller (Plenum, New York, 1975), p. 191.

[8]R. J. H. Clark, in *Advances in Infrared and Raman Spectroscopy,* edited by R. J. H. Clark and R. E. Hester (Wiley, London, 1984), Vol. 11, p. 95.

[9]S. Yamada and R. Tsuchida, Bull. Chem. Soc. Jpn. **29**, 894 (1956).

[10]H. Tanino, J. Nakahara, and K. Kobayashi, in Proceedings of the 15th International Conference on the Physics of Semiconductors, Kyoto, 1980 [J. Phys. Soc. Jpn. **49**, Suppl. A, 695 (1980).

[11]H. Tanino and K. Kobayashi, J. Phys. Soc. Jpn. **52**, 1446 (1983).

[12]K. Nasu, J. Phys. Soc. Jpn. **52**, 3865 (1983).

[13]K. Nasu, J. Phys. Soc. Jpn. **53**, 302 (1984).

[14]K. Nasu, J. Phys. Soc. Jpn. **54**, 1933 (1985).

[15]M. Tanaka, S. Kurita, T. Kojima, and Y. Yamada, Chem. Phys. **91**, 257 (1984).

[16]G. C. Papavassiliou and A. D. Zdetsis, J. Chem. Soc. Faraday Trans. II **76**, 104 (1980).

[17]Y. Wada, T. Mitani, M. Yamashita, and T. Koda, J. Phys. Soc. Jpn. **54**, 3143 (1985).

[18]M. Tanaka, S. Kurita, M. Fujisawa, and S. Matsumoto, J. Phys. Soc. Jpn. **54**, 3632 (1985).

[19]R. J. H. Clark and V. B. Croud, Inorg. Chem. **24**, 588 (1985).

[20]M. Tanaka and S. Kurita, J. Phys. C **19**, 3019 (1986).

[21]M. Tanaka, W. Kaneko, S. Kurita, A. Yamada, and H. Fukutani, J. Phys. Soc. Jpn. **56**, 1197 (1987).

[22]Y. Wada, T. Mitani, M. Yamashita, and T. Koda, Synth. Met. **19**, 907 (1987).

[23]H. Tanino, N. Koshizuka, K. Kobayashi, M. Yamashita, and K. Hoh, J. Phys. Soc. Jpn. **54**, 483 (1985).

[24]H. Tanino, N. Koshizuka, K. Kobayashi, K. Kato, M. Yamashita, and K. Hoh, Physica B + C **139+140B**, 487 (1986).

[25]N. Kuroda, M. Sakai, Y. Nishina, M. Tanaka, and S. Kurita, Phys. Rev. Lett. **58**, 2122 (1987).

[26]M. Tanaka, I. Tsujikawa, K. Toriumi, and T. Ito, Acta Crystallogr. **B38**, 2793 (1982).

[27]H. Tanino, K. Takahashi, M. Kato, and T. Yao, Solid State Commun. **65**, 643 (1988).

[28]M. Haruki, M. Tanaka, and S. Kurita, Synth. Met. **19**, 901

(1987).
[29]A. Kawamori, R. Aoki, and M. Yamashita, J. Phys. C **18**, 5487 (1985).
[30]M. Yamashita, N. Matsumoto, and S. Kida, Inorg. Chim. Acta **31**, L381 (1978).
[31]H. Tanino, H. Oyanagi, M. Yamashita, and K. Kobayashi, Solid State Commun. **53**, 953 (1985).
[32]N. Matsushita, N. Kojima, T. Ban, and I. Tsujikawa, J. Phys. Soc. Jpn. **56**, 3808 (1987).
[33]S. Ichinose, Solid State Commun. **50**, 137 (1984).
[34]Y. Onodera, J. Phys. Soc. Jpn. **56**, 250 (1987).
[35]T. Murao, Phys. Rev. B **35**, 6051 (1987).
[36]D. Baeriswyl and A. R. Bishop, J. Phys. C **21**, 339 (1988).
[37]D. Baeriswyl and A. R. Bishop, Phys. Scr. **T19A**, 239 (1987).
[38]H. Tanino, K. Takahashi, and T. Yao, Jpn. J. Appl. Phys. **25**, L571 (1986).
[39]K. Takahashi, H. Tanino, and T. Yao, Jpn. J. Appl. Phys. **26**, L97 (1987).
[40]H. Tanino, K. Takahashi, and T. Yao, Jpn. J. Appl. Phys. **26**, L983 (1987).
[41]H. Tanino, K. Takahashi, and T. Yao, J. Mol. Electron. **4**, 17 (1988).
[42]N. Elliott and L. Pauling, J. Am. Chem. Soc. **60**, 1846 (1938).
[43]H. Tanino and K. Takahashi, Solid State Commun. **59**, 825 (1986).
[44]L. V. Interrante and F. P. Bundy, J. Inorg. Nucl. Chem. **39**, 1333 (1977).
[45]L. V. Interrante, in *Low-Dimensional Cooperative Phenomena,* edited by H. J. Keller (Plenum, New York, 1975), p. 299.
[46]R. Aoki, Y. Hamaue, S. Kida, M. Yamashita, T. Takemura, Y. Furuta, and A. Kawamori, Mol. Cryst. Liq. Cryst. **81**, 301 (1982).
[47]F. H. Brain, C. S. Gibson, J. A. J. Jarvis, R. F. Phillips, H. M. Powell, and A. Tyabji, J. Chem. Soc. **1952**, 3686 (1952).
[48]K. Takahashi and H. Tanino, Chem. Lett. **1988**, 641 (1988).
[49]K. Takahashi and H. Tanino, Photon Factory Activity Rep. **4**, 1986, p. 176 (unpublished).
[50]F. Herrmann, Ber. Dtsch. Chem. Ges. **38**, 2813 (1905).
[51]G. M. Smith, J. Am. Chem. Soc. **44**, 1769 (1922).
[52]P. C. Ray and D. C. Sen, J. Indian Chem. Soc. **7**, 67 (1930).
[53]H. Tanino, Rev. Sci. Instrum. **57**, 2992 (1986).
[54]M. Tajima, Jpn. J. Appl. Phys. **21**, L227 (1982).
[55]H. B. Gray and C. J. Ballhausen, J. Am. Chem. Soc. **85**, 260 (1963).
[56]H. Tanino, K. Syassen, and K. Takahashi (unpublished).
[57]H. Tanino, M. Holtz, M. Hanfland, K. Syassen, and K. Takahashi (unpublished).
[58]E. A. Allen and W. Wilkinson, Spectrochim. Acta **28A**, 2257 (1972).
[59]K. Takahashi (unpublished).
[60]K. Takahashi and K. Kato, Bull. Chem. Soc. Jpn. **61**, 991 (1988).
[61]B. M. Craven and D. Hall, Acta Crystallogr. **14**, 475 (1961).
[62]N. Matsumoto, M. Yamashita, I. Ueda, and S. Kida, Mem. Fac. Sci., Kyushu Univ. **C11**, 209 (1978).
[63]K. Nasu, M. Yamashita, T. Mitani, and S. Kurita, Butsuri (Proc. Phys. Soc. Jpn.) **41**, 317 (1986) (in Japanese).
[64]See, for example, Y. Toyozawa, in *Excitonic Processes in Solids,* Vol. 60 of Springer Series of *Solid-State Sciences,* edited by M. Ueta, H. Kanzaki, K. Kobayashi, Y. Toyozawa, and E. Hanamura (Springer, Berlin, 1986), p. 245.